Altering the atomic order in nanosized CHA zeolites by post-synthetic silylation treatment

Sajjad Ghojavand, Eddy Dib, Baptiste Riodent, Aymeric Magisson, Valérie Ruaux, Svetlana Mintova

Altering the atomic order in nanosized CHA zeolites by post-synthetic silylation treatment

Sajjad Ghojavand, Eddy Dib, Baptiste Riodent, Aymeric Magisson, Valérie Ruaux, Svetlana Mintova[*]

S. Ghojavand, E. Dib, B. Riodent, A. Magisson, V. Ruaux, S. Mintova
Normandie Université, ENSICAEN, UNICAEN, CNRS, Laboratoire Catalyse et Spectrochimie (LCS), 14000 Caen, France
E-mail: svetlana.mintova@ensicaen.fr

Keywords: nanozeolites, chabazite, dealumination, silylation, post-synthesis treatment

In this work, we present a new post-synthetic hydrothermal approach leading to simultaneous dealumination and silylation of zeolite nanocrystals. Starting from a nanosized chabazite (CHA) type zeolite with a Si/Al ratio equal to 2, a set of samples with Si/Al ratios up to 4 were obtained by altering the acidity and concentration of the added silica modifier during the post-synthesis treatment leading to concurrent dealumination and silylation. The effect of the acidity during the post-synthetic silylation treatment at different pH of 1.0 to 8.5 at a constant silicon concentration was investigated. The nanosized CHA samples were characterized in details by FTIR and NMR spectroscopy (^{1}H, ^{29}Si, ^{27}Al), X-ray diffraction and thermogravimetric analyses. The post-synthesis approach reported here can be applied to other zeolite types for fine tuning of their structural features including type and location of T-atoms, silanol sites and active sites.

1. Introduction

Zeolites are major players in petrochemical industries both for separation and catalysis thanks to their molecular-sized pore openings (0.3–2 nm) and shape selectivity.[1–4] Zeolites consist of ordered corner-sharing TO_4 tetrahedra (T = Si, Al) giving rise to a variety of framework topologies with tunable properties.[5,6] Synthetic zeolites are usually micron-sized polycrystalline powders exhibiting diffusion limitations due to the size of the micropores (0.3-2 nm) and crystals dimensions.[7] These issues were addressed either by hierarchization or by decreasing the zeolite particle size down to nanometer.[8] Thus, nanosized zeolites are advantageous when compared to conventional micron-sized counterparts since they exhibit a higher external surface area, a bigger number of available active sites, and higher diffusion rate.[5,7,9]

Chabazite (CHA) zeolites with Si/Al < 3.0 are excellent CO_2 adsorbents used for separation of CO_2 from CH_4 or N_2 streams thanks to the interaction of CO_2 molecules with the framework Al tetrahedrons.[10–13] However, CHA zeolites with Si/Al > 3.0 are considered for various catalytic applications such as selective catalytic reduction (SCR) of NO_x or methanol to olefins (MTO) reactions.[11]

Conventional syntheses of CHA zeolites involve the use of organic structure-directing agents (OSDAs) (e.g. N,N,N-1-trimethyladamantammonium hydroxide (TMAdaOH)) leading to crystals with a wide Si/Al ratio going from 2.9 to infinity (pure silica).[14–17] Other works reported the use of benzyltrimethylammonium hydroxide (BTMAOH) and tetraethylammonium (TEA) using faujasite (FAU) seeds to synthesize micron-sized high silica CHA crystals.[18,19] However, the economic and environmental concerns are progressively limiting the use of OSDAs in the synthesis of zeolites. This is due to the excessive energy consumption during their own synthesis as well as the CO_2 emission during the removal of templates from the pores by calcination, increasing their carbon finger print in the atmosphere, being non-recyclable.[5,20] Thus, the goal is to develop more sustainable synthesis pathway for nanozeolites without using OSDAs and high crystalline yield.

Typical OSDA-free synthesis routes of CHA are : (i) the inter-zeolite transformation of Al-rich FAU to CHA framework and (ii) the use of a mixture of alkali-metal cations (Na^+, K^+, Cs^+).[20–22] However, both methods give rise to CHA crystals with typical Si/Al ratios around 2.0.[20–22] Alternative protocols were used to synthesize CHA crystals with Si/Al ratios of 4–5 using CHA seeds in addition to Na^+, K^+, and Cs^+ alkali-metal cations.[23] However, TMAdaOH OSDA is still needed for the synthesis of the initial CHA seeds.[23] Other syntheses of CHA crystals with Si/Al ratios of 11–19 were reported using a double seeded

inter-zeolite transformation method using seeds of Si-rich FAU and Al-rich CHA.[21,22,24] However, the final CHA crystals suffer from significant loss of crystallinity.[24]

Alternatively, it is possible to tune the Si/Al ratio of zeolites by post-synthetic dealumination treatment using acids as reported by Barrer.[25] Different acids and salts such as oxalic acids, chromic acids, ammonium fluoride, etc. were employed to leach out Al from different zeolite structures.[26–30] Yet, dealumination with acids leads to significant structural and porosity losses.[31]

In this work, we report a new hydrothermal post-synthetic treatment consisting of a concurrent silylation and dealumination towards increase the Si/Al ratio of nanosized CHA zeolites synthesized free of OSDAs. The starting CHA nanozeolite with a Si/Al ratio of 2.0 is subjected to hydrothermal post-synthetic treatment at different conditions (pH of 8.5, 2.4, and 1.0) in the presence of tetraethyl orthosilicate (TEOS) added to silylate the samples with two different concentrations (2 or 4 mmol g^{-1}). The structural features and chemical compositions of the nanosized CHA were characterized by spectroscopic and diffraction approaches. By the new post-synthetic approach, nanosized CHA zeolites with low Al content without utilizing OSDAs can be synthesized. This directly reduces the CO_2 emission of energy intensive calcination step needed to remove OSDAs which is in accordance with the 13th United Nations' goal in sustainable development (SDG 13) to combat climate change.[32] The zeolites are important catalysts and sorbents, therefore the sustainable synthesis free of organic templates with high crystalline yield is of interest to ensure access to affordable and sustainable energy (SDG 7).[32]

2. Results and discussion

Six nanosized CHA samples ($2.0 < Si/Al < 4.0$) were prepared by hydrothermal post-synthetic treatment of the reference nanosized CHA zeolite sample (Si/Al = 2.0) synthesized according to the procedure developed by our group.[13,20] The structural details of the nanosized CHA samples are presented in Table 1 and Table S1. Based on the conditions of silylation, the samples were labeled as CHA-pHα-βSi; where α is the pH of the silylation solution, and β is the TEOS/zeolite ratio in mmol g^{-1} of zeolite.

Table 1. Silylated nanosized CHA samples obtained by hydrothermal post-synthetic treatment approach: Si/Al ratio, silanol concentrations, and degree of crystallinity.

Sample	pH	Si concentration /mmol g^{-1}	Si/Al FTIR	Si/Al NMR	Si/Al ICP	$[OH]_{FTIR}$ cm^{-1} g^{-1}	$[OH]_{NMR}$ mmol g^{-1}	Crystallinity[a] /%
Reference	-	-	2.1	2.0	2.2	644	3.43	100
CHA-pH8.5-2Si	8.5	2.3	2.5	2.5	2.7	1296	3.99	100
CHA-pH8.5-4Si	8.5	4.6	2.6	2.8	2.9	1427	4.14	98
CHA-pH2.4-2Si	2.4	2.3	2.2	2.3	2.4	1756	5.62	98
CHA-pH2.4-4Si	2.4	2.3	2.7	2.8	3.0	1743	5.60	97
CHA-pH1.0-2Si	1.0	2.3	3.3	3.7	3.8	3331	6.61	79
CHA-pH1.0-4Si	1.0	4.6	3.7	4.0	4.0	2831	6.36	41

[a] Crystallinity was determined based on XRD diffraction data (peaks at 9.4 and 12.8° 2θ were used) the reference sample with 100% crystallinity was used from[20].

To study the effect of the acidity during the silylation steps, the pH of the solutions was varied from 8.5 to 1.0 by keeping the Si concentration constant (2 or 4 mmol g^{-1}). Firstly, two experiments were performed without adding TEOS as the silylation agent at pH of 8.5 and 1.0 to obtain samples CHA-pH8.5 and CHA-pH1.0, respectively. As shown in **Figure S2**, the CHA-pH8.5 sample preserved its crystallinity after the post-synthetic treatment, while an amorphous phase alongside the CHA crystalline phase started to appear in sample CHA-pH1.0. When 2 mmol g^{-1} of Si were added to the samples during the silylation step, the obtained CHA-pH8.5-2Si and CHA-pH2.4-2Si nanosized samples preserved their crystallinity (100 and 98 %,) compared to the reference nanosized CHA (**Figure 1a** and Table 1) while the Si/Al ratio increased to 2.7 and 2.4 based on ICP-MS study. The water content reduced from 17.7 to 15.2 and 15.7 % for samples CHA-pH8.5-2Si and CHA-pH2.4-2Si, respectively, compared to the reference material (**Figure 1a**, **Figure S1**, and Table 1). However, decreasing the pH value of the silylation solution to 1.0 for the preparation of sample CHA-pH1.0-2Si resulted in 21% loss of crystallinity and the Si/Al ratio increased to 3.8 while the water content decreased to 12.9 % (**Figure 1a**, **Figure S1**, and Table 1). Further, under treatment of nanosized CHA zeolite with increased Si concentration (4 mmol g^{-1}) at different pH values (samples CHA-pH8.5-4Si, CHA-pH2.4-4Si, and CHA-pH1.0-4Si) the same trends for the Si/Al ratio and degree of crystallinity were observed (**Figure 1a**, **Figure S1**, and Table 1).

The structural features of the nanosized CHA samples were revealed by FTIR using KBr pellet technique (**Figure 1b**). All samples show two distinct peaks at 518 and 635 cm^{-1}, attributed to the double six-membered rings (*d6r*) and eight-membered rings (8MRs) of CHA framework.[20] These peaks with high intensity are well resolved for all samples except for those treated at pH of 1.0, thus reflecting the decrease of crystallinity (Table 1). Furthermore, the O–Si–O bending mode at 466 cm^{-1} is observed for all samples.[33,34] Two broad vibration bands, the first at 670–820 cm^{-1} related to the symmetric vibration of Si–O–T (T = Al or Si)

and the second one at 950-1200 cm^{-1} related to the asymmetric stretching are also recorded for all samples.[35–38] The asymmetric stretching band assigned to Si–O–T associated with variation of the Si/Al ratio of the samples is shifted too.[35] The Si/Al ratio of the samples determined based on the FTIR data is in a good agreement with the ICP-MS results (**Figure 1b** and Table 1).

The state of Al in the zeolite samples was studied by ^{27}Al MAS NMR and the results are presented in **Figure S3**. A unique peak at 57.7 ppm corresponding to the tetrahedrally coordinated Al similarly to the reference sample is observed (Table 1).[1,20] However, for the samples treated at pH of 1.0 (CHA-1.0-2Si and CHA-1.0-4Si), a small peak at 0 ppm related to extra-framework Al species appeared. This explains the decrease of crystallinity for the samples. Similar results for FAU zeolite post-synthetically treated by HCl under low pH values were reported earlier.[39]

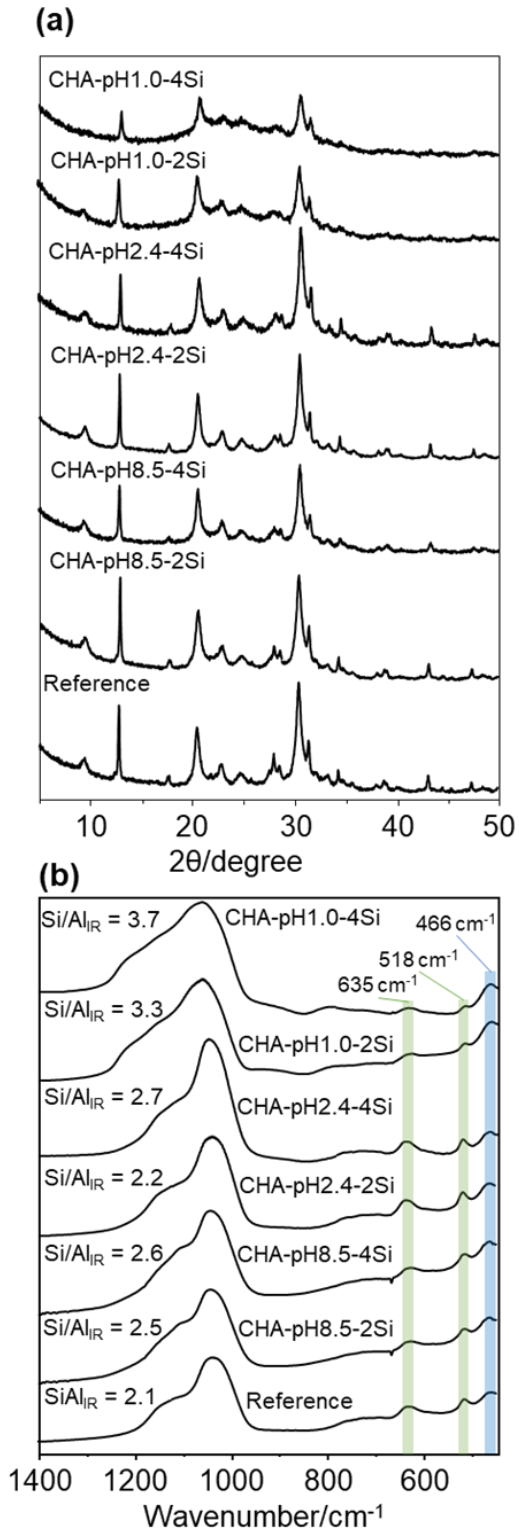

Figure 1. (a) XRD patterns, and (b) IR spectra using KBr method of nanosized CHA reference, CHA-pH8.5-2Si, CHA-pH8.5-4Si, CHA-pH2.4-2Si, CHA-pH2.4-4Si, CHA-pH1.0-2Si, and CHA-pH1.0-4Si samples.

^{29}Si MAS NMR spectra of nanosized CHA samples and the corresponding percentage of different Q^n species (n = number of Si atoms surrounding a SiO_4 tetrahedron) are presented in

Figure 2, **Figure S2, Figure S4a**, and **Table S2**. All samples display five distinct resonances at -89, -94, -99, -104, and -109 ppm corresponding to the five crystallographic SiO_4 sites coordinated by either Al^{3+} or hydroxyl groups assigned to Q^{0-4} species.[13,20,40] The Si/Al ratio of all samples was determined using Engelhardt and Michel equation and the results are shown in Table 1.[41]

Interestingly, the treatment of the CHA zeolite with 2 mmol g^{-1} of Si under basic condition (sample CHA-pH8.5-2Si), gives rise to a new peak at -113 ppm assigned to Q^4 species (**Figure 2** and **Figure S4a**).[42] Both resonances at -109 and -113 ppm correspond to Q^4 species, however, the Si–O–Si angle of these two sites may be slightly different as estimated to be equal to 146 and 148°, respectively.[42–44] The resonance at -113 ppm is not present in sample CHA-pH8.5 when the silylation agent (TEOS) was not added during the post-synthetic treatment (**Figure S2**).

Increasing the amount of silylation agent to 4 mmol g^{-1} during basic post-synthetic treatment (sample CHA-pH8.5-4Si) results in further development of new Q^4 species at -113 ppm; the Si/Al ratio of this sample increased to 2.8 (Table 1). Comparing the reference sample to CHA-pH8.5-2Si reveals that the increase of the Si/Al ratio of the post-synthetically treated sample in basic condition from 2 to 2.5 is due to the formation of Q^4 species at -113 ppm. Increasing the dosage of the silylation agent from 2 to 4 mmol g^{-1} in samples CHA-pH8.5-2Si and CHA-8.5-4Si gives rise to a further development of these species and a consequent increase of the Si/Al ratio from 2.5 to 2.8, respectively (Table 1). Thus, the band at -113 ppm is characteristic of new Si tetrahedra inserted into to the framework during the silylation step.

In acidic conditions at pH of 2.4, the CHA-pH2.4-2Si sample contains a single Q^4 resonance at -109 ppm similar to the reference CHA sample (**Figure 2** and **Figure S4a**). However, the Si/Al ratio of the CHA-pH2.4-2Si sample increases to 2.3 (see Table 1). The increase of the Si/Al ratio is due to the decrease in the concentration of Q^{0-2} species attributed to Al etching in acidic media.[26,27,45] Increasing the dosage of silylation agent from 2 to 4 mmol g^{-1} at the same pH (samples CHA-pH2.4-2Si vs CHA-pH2.4-4Si) results in further evolution of the Si/Al ratio from 2.3 to 2.8, respectively (**Figure 2**). The new resonance at -113 ppm assigned to slightly different coordinated Q^4 species are also observed in the spectrum of CHA-pH2.4-4Si sample. The deconvoluted spectra of CHA-pH2.4-2Si and CHA-pH2.4-4Si samples reveal the reduction of Q^1 species from 18 to 9 % and increase of Q^4 species from 4 to 18 %, respectively. These results suggest that during the silylation, a simultaneous dealumination occurred in the samples.

Under harsh acidic condition (pH = 1.0), the CHA-pH1.0-2Si sample reached a Si/Al ratio of 3.7 as determined by ^{29}Si MAS NMR (**Figure 2** and Table 1). The concentration of Q^1 species decreases from 20 to 3 % due to the dealumination.[26,27,45] Moreover, similar dealumination was observed for sample CHA-pH1.0 obtained under treatment without using the silylation agent (TEOS) (**Figure S2**). The concentration of Q^4 species increased from 15 % for CHA-pH1.0 to 33 % for CHA-pH1.0-2Si thus proving the simultaneous dealumination and silylation of the samples when TEOS was used during the post-synthetic treatment. In addition, increasing the amount of the silylation agent to 4 mmol g^{-1} results in further increase in Si/Al ratio to 4.0 for sample CHA-pH1.0-4Si. The silylation degree of CHA-pH1.0-4Si sample is similar to that of CHA-pH1.0-2Si sample, however, the resolution of the ^{29}Si resonances noticeably decrease that can be due to the partial amorphization of sample CHA-pH1.0-4Si; this has been approved by XRD characterization of the sample (**Figure 1**, **Figure 2**, and Table 1).

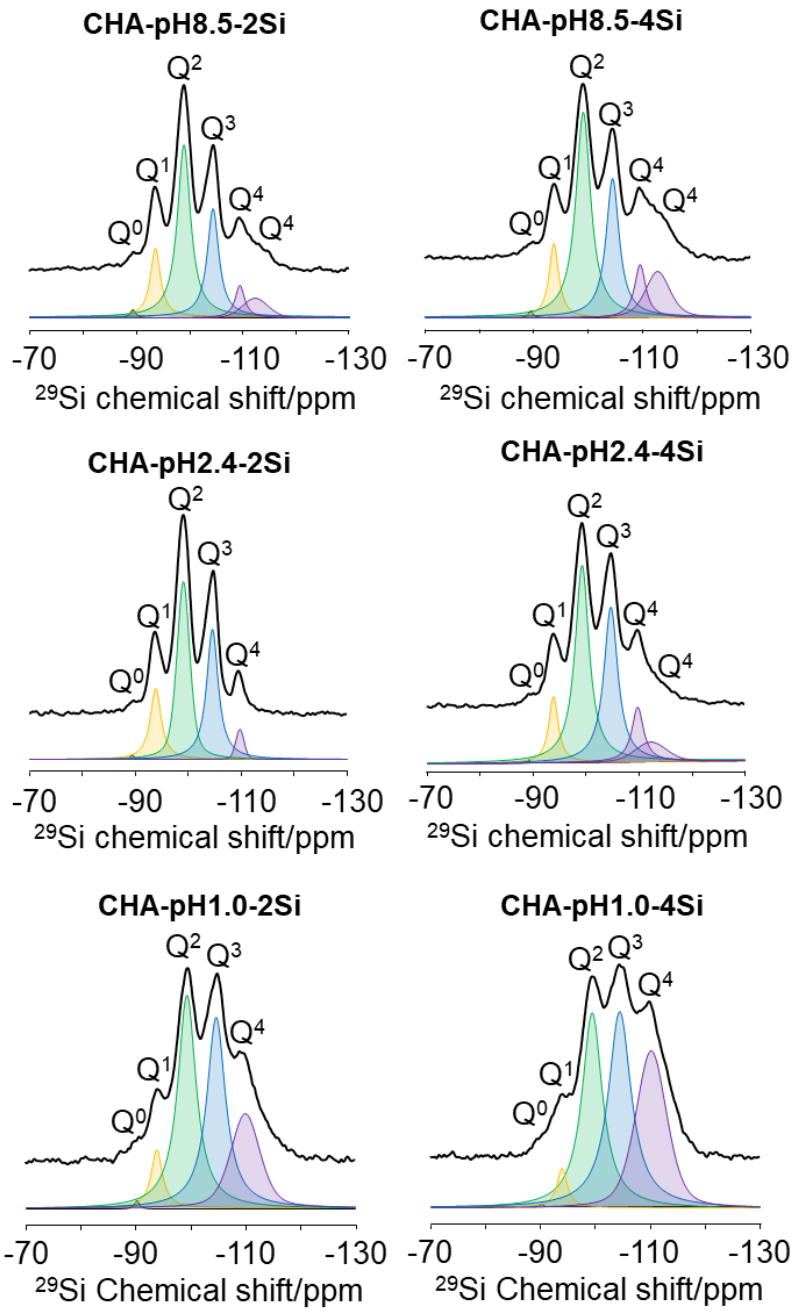

Figure 2. ^{29}Si MAS NMR spectra of CHA-pH8.5-2Si, CHA-pH8.5-4Si, CHA-pH2.4-2Si, CHA-pH2.4-4Si, CHA-pH1.0-2Si, and CHA-pH1.0-4Si nanosized CHA samples. Color code: black for Q^0, yellow for Q^1, green for Q^2, blue for Q^3, and purple for Q^4 species.

Figure 3 presents the changes in the percentages of different $Q^{1\text{-}4}$ species after silylation/dealumination of samples at various pH using variable Si concentrations. When 2 mmol g^{-1} of Si is inserted, all samples show a decrease in the amount of $Q^{1\text{-}2}$ species due to dealumination and an increase in the amount of $Q^{3\text{-}4}$ species due to silylation. In addition, increasing the Si concentration from 2 to 4 mmol g^{-1} significantly increases the amount of Q^4 species (**Figure 3**), hence, decreasing $Q^{1\text{-}3}$ species percentage for all samples. The percentage

of Q^2 species clearly decreases by reducing the pH level from 8.5 to 1.0, which is in line with previous works[26,27] while no clear trends were observed for the $Q^{1,3,4}$ species. These simultaneous changes in the distribution of the Q^n species provide an evidence for the occurrence of a concurrent dealumination and silylation mechanism with a substantial introduction of Si resulting in the formation of new Q^4 species.

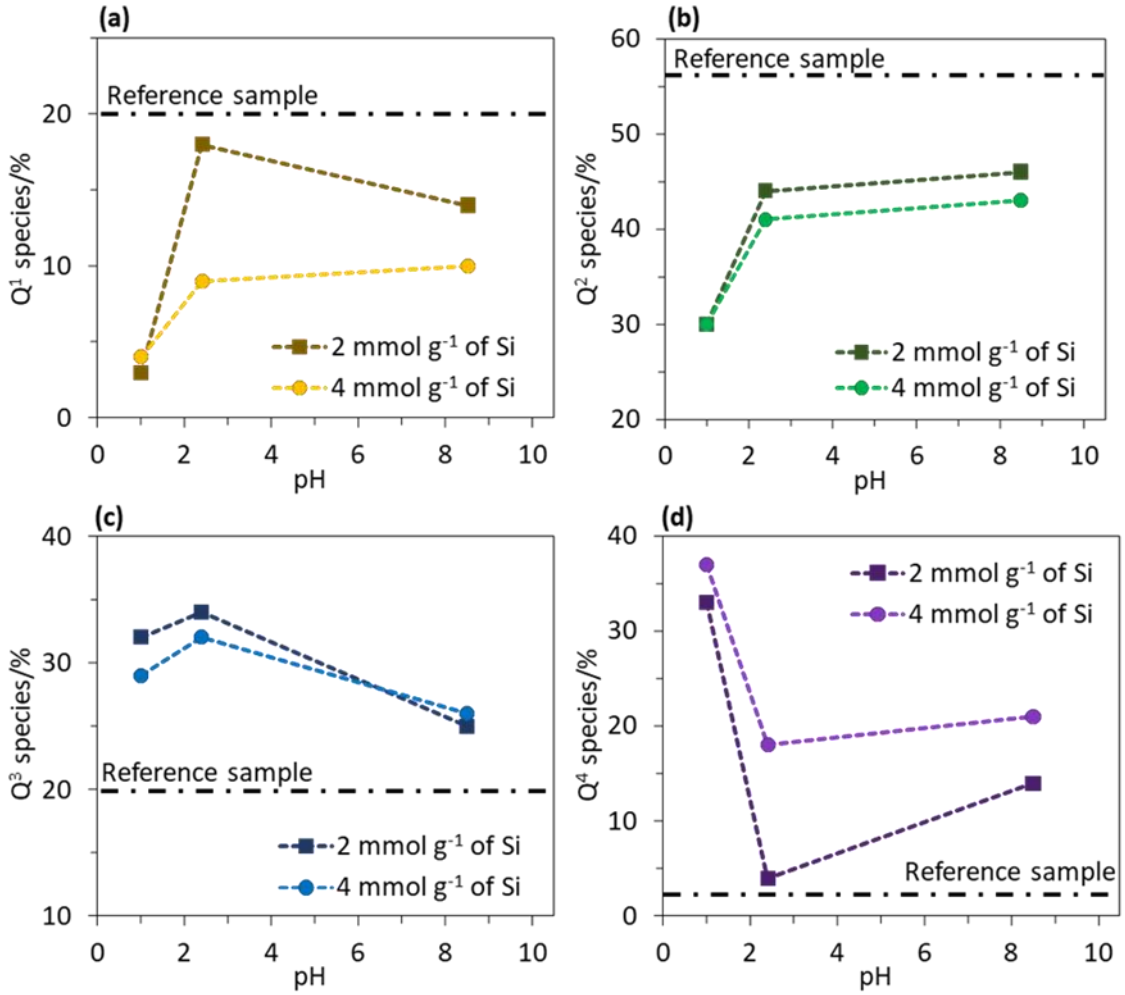

Figure 3. The changes in (a) Q^1, (b) Q^2, (c) Q^3, and (d) Q^4 species versus the pH and Si concentration during the post-synthetic treatment of nanosized CHA based on ^{29}Si MAS NMR spectroscopy characterization.

The Q^n species, being assigned to different coordination of Si may originate from the presence of Al or OH groups equally and it is difficult to be distinguished using only ^{29}Si NMR spectroscopy. Hence, high resolution ^{1}H MAS NMR spectra were acquired for all CHA samples dehydrated at 350 °C in order to estimate the amount of silanol sites before and after treatment (**Figure 4**, **Figure S4b**, and Table S3). The concentrations of silanol groups for

these samples are summarized in Table 1. Four distinct regions are identified: (i) silanol groups close to cations (in purple) represented by O–H stretching vibrations appearing in the range of 3766–3756 cm^{-1} of the FTIR, and negative values for proton chemical shifts, (ii) isolated or weakly hydrogen bonded silanol sites (in blue) in the range of 3756–3700 cm^{-1}, and proton chemical shift at 0.0–2.0 ppm, (iii) moderately hydrogen bonded silanol sites (in yellow) in the range of 3700–3470 cm^{-1}, and proton chemical shift at 2.0–4.5 ppm, and (iv) strongly hydrogen bonded silanol sites (in red) in the range of 3470–3100 cm^{-1}, and proton chemical shifts above 4.5 ppm.[46]

The silanol groups were also characterized using FTIR spectroscopy, the O–H stretching region of the spectra are presented in **Figure 5**, and the full spectra are plotted in **Figure S5** . The spectra show a wide range of silanol sites from 3100 to 3800 cm^{-1} (**Figure 5**). Exact identification and deconvolution of the different silanol sites is not obvious using FTIR spectroscopy due to the complex nature of O–H stretching vibrations in this region. Hence, the different silanol sites using ^{1}H MAS NMR spectroscopy were studied adapting the methodology established earlier.[46,47] The total concentration of the silanol sites by integration of the entire band area of 3100–3756 cm^{-1} was estimated (**Table 1**).

Upon adding 2 mmol g^{-1} Si during the silylation step in basic conditions (sample CHA-pH8.5-2Si), the total amount of silanol sites increases by 16%, i.e. from 3.43 to 3.99 mmol g^{-1}, and the new silanols are found to be mainly isolated (**Figure 4a**, and Table S3, Table 1). Increasing the Si amount to 4 mmol g^{-1} under basic conditions (sample CHA-pH8.5-4Si) increases the moderately hydrogen bonded silanol groups concentration by 29 %, i.e. from 3.43 to 4.14 mmol g^{-1}, while the peak corresponding to the strongly hydrogen bonded silanol sites disappears (**Figure 4b** and Table 1). Then, for both CHA-pH8.5-2Si and CHA-pH8.5-4Si samples, the dealumination was found to create more silanol sites. The same trend is observed for the total concentration of silanol sites determined by integration of the silanol region of the FTIR spectra (**Figure 5** and Table 1).

Upon addition of 2 mmol g^{-1} Si at pH of 2.4, the total silanol sites concentration increases by 64%, i.e. from 3.43 to 5.62 mmol g^{-1} as determined by ^{1}H MAS NMR spectroscopy and FTIR using from 840 to 1756 cm^{-1} g^{-1} (reference samples vs CHA-pH2.4-2Si; Table 1). Similarly, to the basic treatment, the concentration of the isolated and moderately hydrogen bonded silanol sites (blue and yellow peaks) increases for sample CHA-pH2.4-2Si, while strongly hydrogen bonded silanol groups (red peaks) are not observed as compared to the reference sample (**Figure 4c**). Increasing the amount of Si to 4 mmol g^{-1} (sample CHA-pH2.4-4Si) leaded to the formation of silanol sites with similar concentration (5.60 mmol g^{-1}) based on ^{1}H MAS

NMR and FTIR (1743 cm^{-1} g^{-1}) in comparison to sample CHA-pH2.4-2Si (Table 1 and **Figure 4c,d**).

In samples CHA-pH1.0-2Si and CHA-pH1.0-4Si, the total amount of silanol groups reaches 6.61 mmol g^{-1} and 6.36 mmol g^{-1}, respectively based on ^{1}H MAS NMR and FTIR (Table 1). Approximately 40 % of these silanol groups are isolated or weakly hydrogen bonded and the rest are moderately hydrogen bonded (Figure 4e,f). The global changes in the silanol groups concentration of the samples after silylation steps at various pH and Si concentrations are presented in **Figure S6**. The isolated silanol sites, weakly and moderately hydrogen bonded are influenced by the pH of the treating solutions rather than the Si amount added. Decreasing the pH from 8.5 to 1.0 results in more than 350% increase in moderately hydrogen bonded silanol groups. The dealumination at low pH leads to the formation of these silanol sites without any reorganization of Al species in the framework. The post-synthesis treatment significantly changes both the Si/Al ratio and subsequently the silanol sites concentration even when the amount of Q^4 sites increased (Table 1, **Figure 3**, **Figure 4**, and **Figure 5**). This is another proof that a simultaneous dealumination and silylation occurred in the samples.

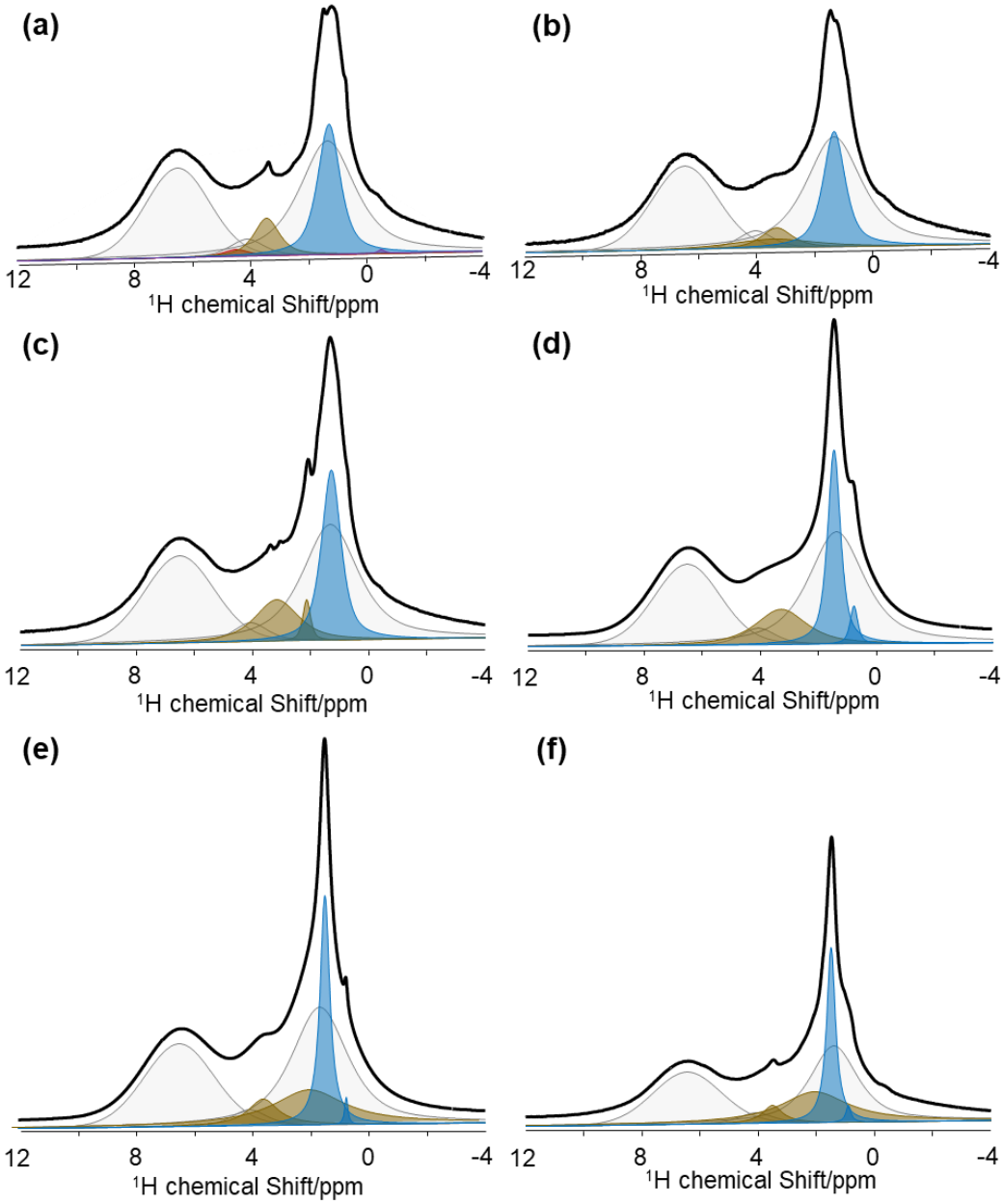

Figure 4. ^{1}H MAS NMR spectra of (a) CHA-pH8.5-2Si, (b) CHA-pH8.5-4Si, (c) CHA-pH2.4-2Si, (d) CHA-pH2.4-4Si, (e) CHA-pH1.0-2Si, and (f) CHA-pH1.0-4Si zeolite samples. Color code: rotor signals in grey, purple for silanol sites interacting with cations, blue for isolated and weakly hydrogen bonded, yellow for moderately hydrogen bonded, and red for strongly hydrogen bonded silanol groups.

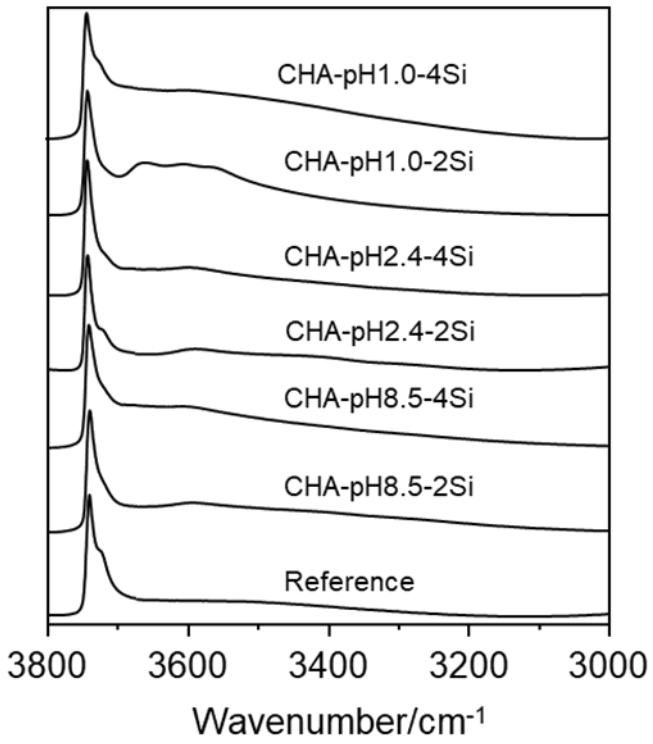

Figure 5. FTIR spectra representing the silanol region (3000-3800 cm^{-1}) of reference, CHA-pH8.5-2Si, CHA-pH8.5-4Si, CHA-pH2.4-2Si, CHA-pH2.4-4Si, CHA-pH1.0-2Si, and CHA-pH1.0-4Si zeolite samples.

The pH and amount of Si used for the post-synthesis treatment of the CHA zeolite with Si/Al ratio of 2.0 leaded to significant change of both the Si/Al ratio and silanol sites concentration of the samples. Performing the post-synthesis silylation steps under basic conditions (pH = 8.5) resulted in samples CHA-pH8.5-2Si and CHA-pH8.5-4Si with Si/Al ratios of 2.5 and 2.8, respectively as determined by ^{29}Si MAS NMR (**Figure 2** and Table 1). Both samples preserved the high crystallinity as shown by XRD patterns (**Figure 1a**), ^{27}Al MAS NMR spectra with the symmetrical band at 57.7 ppm (**Figure S3**), and IR spectra with two structural bands at 518 and 635 cm^{-1} (**Figure 1b**).[20] ^{29}Si MAS NMR spectroscopy revealed that in addition to the Q^4 species detectable in the reference CHA sample (^{29}Si chemical shift of -109 ppm), new Q^4 species at -113 ppm for samples CHA-pH8.5-2Si and CHA-pH8.5-4Si responsible for the higher Si/Al ratio of 2.5 and 2.8, respectively are appeared. The new Q^4 species are originated from the insertion of Si in the CHA framework during the post-synthetic treatment step. The ^{1}H MAS NMR spectroscopy revealed that the silylation step heals the strongly hydrogen bonded silanol sites observable at 4.5 ppm (**Figure 4**). The FTIR results in estimating the total amount of silanol sites for CHA-pH8.5-2Si and CHA-pH8.5-4Si samples determined by FTIR are in a good agreement with ^{1}H MAS NMR results; an almost

constant molar absorption coefficient of 650 cm $mmol^{-1}$ calculated for these samples is presented in Table S1. Performing the post-synthesis silylation steps under pH of 2.4 also resulted in fully crystalline nanosized CHA samples (CHA-pH2.4-2Si and CHA-pH2.4-4Si) as supported by XRD patterns, ^{27}Al MAS NMR, and IR (**Figure 1** and **Figure S3**). The Si/Al ratios can be tuned to 2.3 and 2.8 for CHA-pH2.4-2Si and CHA-pH2.4-4Si samples, respectively (**Figure 2**). While the total silanols concentration is ~5.60 mmol g^{-1} for both CHA-pH2.4-2Si and CHA-pH2.4-4Si samples. Finally, it was found that performing the post-synthesis silylation steps on the nanosized CHA samples under low pH of 1.0 still preserve of about 79% and 41% crystallinity of samples CHA-pH1.0-2Si and CHA-pH1.0-4Si, respectively (**Figure 1a** and Table 1). This agrees with detection of a resonance at 0 ppm in the ^{27}Al NMR corresponding to octahedrally coordinated Al in the samples and addition of anisotropy to the tetrahedral ^{27}Al resonance at 57.7 ppm (**Figure S3**). Nevertheless, the final Si/Al ratios of 3.7 and 4.0 for CHA-pH1.0-2Si and CHA-pH1.0-4Si samples using ^{29}Si MAS NMR spectroscopy were estimated (**Figure 2**).

3. Conclusions

The effect of pH and the amount of Si source used for post-synthetic hydrothermal treatment of nanosized chabazite crystals with initial Si/Al ratio of 2.0 was studied systematically. The nanosized CHA with Si/Al ratios between 2.0–4.0 and defect site concentrations of 3.43 to 6.61 mmol g^{-1} were prepared. Detailed spectroscopic characterization by FTIR, ^{1}H, ^{27}Al, and ^{29}Si MAS NMR spectroscopy were performed to characterize the amount and type of defect sites and local environment of different nuclei within the zeolite (i.e. H, Al, and Si) after the post-synthetic hydrothermal treatment. ^{29}Si MAS NMR spectroscopy revealed the increase of the Si/Al ratio of the samples are due to the decrease of Q^{0-2} species (dealumination) and increase of Q^4 species due to the Si insertion as characterized by the newly formed Q^4 species at -113 ppm.

All strongly hydrogen bonded silanols were healed during the post-synthetic hydrothermal treatment as revealed by ^{1}H MAS NMR spectroscopy. While, the total silanol groups concentration increased due to the constant dealumination and silylation of the samples; mainly isolated silanol groups or weak/medium hydrogen bonded silanol groups were formed. The silanol groups generated in the samples strongly depend on the pH conditions and not on the Si concentration used during the post-synthesis treatment.

Herein, a potentially universal method for a concurrent dealumination and silylation of zeolites is presented that can be extended to other zeolitic types providing control over zeolite's structural features such as T-atoms and active sites.

4. Experimental section

4.1. Materials and synthesis

The reference nanosized CHA sample with a Si/Al ratio of 2.0 was synthesized using the procedure reported previously.[20] In a typical synthesis, 0.54 g of $NaAlO_2$, 1.7 g of NaOH, 0.824 g of KOH, 0.442 g of CsOH (50 wt.% Cs in water), and 4.2 g of water were initially mixed to obtain a clear solution. Then, 10 g of LUDOX AS-40 was added dropwise under vigorous stirring (final gel composition of 0.2 Cs_2O: 1.5 K_2O: 6.0 Na_2O: 16.0 SiO_2: 0.7 Al_2O_3: 141.7 H_2O) and aged for 17 days at ambient conditions. Afterwards, the sample was hydrothermally treated at 90 °C for 7 h and the CHA nanocrystals synthesized were purified and washed by double-distilled (dd) water and recovered by centrifugation. The samples were dried at 60 °C overnight and labeled as the reference nanosized CHA (composition: $Na_{1.8}K_{5.7}Cs_{4.0}Al_{11.1}Si_{24.8}O_{72}$) prior post-synthesis treatment and characterization.

Prior the post-synthetic treatment of CHA zeolite, 0.45–0.90 mmol of tetraethyl orthosilicate (TEOS, Sigma-Aldrich 98 wt %) with 3 g of milli-Q water was hydrolyzed at ambient conditions for 2 h; the pH was adjusted using ammonia (Sigma-Aldrich, 25 wt %) or hydrochloric acid (VWR chemicals, 37 wt %). 200 mg of the reference nanosized CHA sample was added to the pre-hydrolyzed TEOS solutions under stirring and then added into autoclaves for further hydrothermal treatment for 24 h at 90 °C. Additionally, two experiments were performed where the nanosized CHA was only treated with ammonia at pH of 8.5 or hydrochloric acid at pH of 1.0 without the use of TEOS reagent. Finally, the post-treated samples were purified by three cycles of centrifugation and washing with dd water followed by drying at 60 °C overnight.

4.2. Characterization

Powder X-ray diffraction (XRD) patterns of the zeolite samples were collected with a PANalytical X'Pert Pro diffractometer using Cu-Kα1 radiation (λ = 1.5406 Å, 45 kV, 40 mA). Inductively coupled plasma mass spectrometry (ICP-MS) measurements were performed using a 7900 ICP-MS from Agilent Technologies. Thermogravimetric analysis (TG) was performed using a TAG24 SETARAM analyzer under a N_2 atmosphere. Measurements were performed between 30 and 800 °C with a ramp rate of 1 °C min^{-1}.

Magic-angle spinning nuclear magnetic resonance (MAS NMR) spectra of ^{29}Si and ^{27}Al nuclei were recorded with a single pulse on a Bruker Avance 500 MHz (11.7 T) spectrometer using 4 mm-OD zirconia rotors with a spinning frequency of 12 and 14 kHz, respectively. Single pulse excitation (30° and 15° flip angle) of 3 μs was used for ^{29}Si and ^{27}Al MAS NMR experiment and 30 s of recycle delay. Tetra-methylsilane (TMS) and $Al(NO_3)_3$ were used as references for ^{29}Si and ^{27}Al nuclei, respectively. One dimensional ^{1}H MAS NMR spectra were acquired using 1.9 mm outer diameter probes zirconia rotors spun at 40 kHz, a radiofrequency power of 114 kHz and a recycle delay of 10 s. The fitting of ^{1}H and ^{29}Si MAS NMR spectra was performed using Lorentzian peaks in Dmfit software.[48]

Fourier transform infrared (FTIR) spectroscopic measurements of zeolite samples were performed on a self-supported pellet (~20 mg and a diameter of 16 mm); the transmission spectra were recorded with a Thermo Scientific Nicolet iS50 FTIR spectrometer equipped with an MCT detector, at a spectral resolution of 4 cm^{-1}. The FTIR cell is equipped with a heating element in order to activate the samples at 350 °C prior to the measurements. The cell was connected to a pumping system for the treatment under high vacuum (up to 10^{-6} kPa). The samples were activated by heating with a ramp rate of 3 °C min^{-1} followed by heating at 350 °C for 4 h under high vacuum. All IR spectra were recorded at room temperature. The structural features of zeolites samples were identified by FTIR using samples prepared with KBr (1 mg of CHA samples and 99 mg of KBr); the structural fingerprints of zeolites are observed in the range 1400–450 cm^{-1}. The Si/Al ratio of nanosized CHA samples were also calculated using the modified empirical equation of Ma et al. as $Si/Al_{IR} = (0.0458*\nu)-45.587$, where ν is the position of asymmetric stretching of Si–O–T (T = Si or Al) in cm^{-1}.[35]

Supporting Information

Supporting Information is available from the Wiley Online Library or from the author.

Acknowledgements

Financial support from the Normandy Region through the Label of Excellence for the Centre of Zeolites and Related Nanoporous Materials by the Region of Normandy is acknowledged.

Received: ((will be filled in by the editorial staff))
Revised: ((will be filled in by the editorial staff))
Published online: ((will be filled in by the editorial staff))

References

[1] J. Shang, G. Li, R. Singh, Q. Gu, K. M. Nairn, T. J. Bastow, N. Medhekar, C. M. Doherty, A. J. Hill, J. Z. Liu, P. A. Webley, *J. Am. Chem. Soc.* **2012**, *134*, 19246.

[2] S. V. Konnov, F. Dubray, E. B. Clatworthy, C. Kouvatas, J.-P. Gilson, J.-P. Dath, D. Minoux, C. Aquino, V. Valtchev, S. Moldovan, S. Koneti, N. Nesterenko, S. Mintova, *Angew. Chem. Int. Ed. n/a*.

[3] J. Grand, N. Barrier, M. Debost, E. B. Clatworthy, F. Laine, P. Boullay, N. Nesterenko, J.-P. Dath, J.-P. Gilson, S. Mintova, *Chem. Mater.* **2020**, *32*, 5985.

[4] S. Mintova, E. B. Clatworthy, S. V. Konnov, F. Dubray, N. Nesterenko, J.-P. Gilson, *Angew. Chem. Int. Ed. n/a*.

[5] S. Mintova, J.-P. Gilson, V. Valtchev, *Nanoscale* **2013**, *5*, 6693.

[6] E. Koohsaryan, M. Anbia, *Chin. J. Catal.* **2016**, *37*, 447.

[7] L. Tosheva, V. P. Valtchev, *Chem. Mater.* **2005**, *17*, 2494.

[8] S. Mintova, J. Grand, V. Valtchev, *Comptes Rendus Chim.* **2016**, *19*, 183.

[9] G.-T. Vuong, T.-O. Do, In *Mesoporous Zeolites*, John Wiley & Sons, Ltd, **2015**, pp. 79–114.

[10] J. Shang, G. Li, R. Singh, P. Xiao, J. Z. Liu, P. A. Webley, *J. Phys. Chem. C* **2013**, *117*, 12841.

[11] M. Dusselier, M. E. Davis, *Chem. Rev.* **2018**, *118*, 5265.

[12] K. Chen, S. H. Mousavi, R. Singh, R. Q. Snurr, G. Li, P. A. Webley, *Chem. Soc. Rev.* **2022**, *51*, 1139.

[13] S. Ghojavand, B. Coasne, E. B. Clatworthy, R. Guillet-Nicolas, P. Bazin, M. Desmurs, L. Jacobo Aguilera, V. Ruaux, S. Mintova, *ACS Appl. Nano Mater.* **2022**, *5*, 5578.

[14] Y. Guo, T. Sun, Y. Gu, X. Liu, Q. Ke, X. Wei, S. Wang, *Chem. - Asian J.* **2018**, *13*, 3222.

[15] S. I. Zones, *J. Chem. Soc. Faraday Trans.* **1991**, *87*, 3709.

[16] E. A. Eilertsen, B. Arstad, S. Svelle, K. P. Lillerud, *Microporous Mesoporous Mater.* **2012**, *153*, 94.

[17] J. R. Di Iorio, R. Gounder, *Chem. Mater.* **2016**, *28*, 2236.

[18] M. Itakura, T. Inoue, A. Takahashi, T. Fujitani, Y. Oumi, T. Sano, *Chem. Lett.* **2008**, *37*, 908.

[19] N. Martín, M. Moliner, A. Corma, *Chem. Commun.* **2015**, *51*, 9965.

[20] S. Ghojavand, E. B. Clatworthy, A. Vicente, E. Dib, V. Ruaux, M. Debost, J. El Fallah, S. Mintova, *J. Colloid Interface Sci.* **2021**, *604*, 350.

[21] J. Shang, G. Li, R. Singh, P. Xiao, J. Z. Liu, P. A. Webley, *J. Phys. Chem. C* **2010**, *114*, 22025.

[22] M. Bourgogne, J.-L. Guth, R. Wey, *Process for the preparation of synthetic zeolites, and zeolites obtained by said process*, **1985**.

[23] H. Imai, N. Hayashida, T. Yokoi, T. Tatsumi, *Microporous Mesoporous Mater.* **2014**, *196*, 341.

[24] S. Goel, S. I. Zones, E. Iglesia, *Chem. Mater.* **2015**, *27*, 2056.

[25] R. M. Barrer, M. B. Makki, *Can. J. Chem.* **1964**, *42*, 1481.

[26] C. W. Jones, S.-J. Hwang, T. Okubo, M. E. Davis, *Chem. Mater.* **2001**, *13*, 1041.

[27] Z. Qin, L. Hafiz, Y. Shen, S. V. Daele, P. Boullay, V. Ruaux, S. Mintova, J.-P. Gilson, V. Valtchev, *J. Mater. Chem. A* **2020**, *8*, 3621.

[28] V. Valtchev, G. Majano, S. Mintova, J. Pérez-Ramírez, *Chem. Soc. Rev.* **2012**, *42*, 263.

[29] V. Babić, S. Koneti, S. Moldovan, M. Debost, J.-P. Gilson, V. Valtchev, *Microporous Mesoporous Mater.* **2022**, *329*, 111513.

[30] E. B. Lami, F. Fajula, D. Anglerot, T. Des Courieres, *Microporous Mater.* **1993**, *1*, 237.

[31] C.-Y. Chen, S. I. Zones, In *Zeolites and Catalysis*, John Wiley & Sons, Ltd, **2010**, pp. 155–170.

[32] UN's Sustainable Developement Goals, United Nations, **2020**.

[33] E. M. FLANIGEN, H. KHATAMI, H. A. SZYMANSKI, In *Molecular Sieve Zeolites-I*, AMERICAN CHEMICAL SOCIETY, **1974**, pp. 201–229.
[34] X. Guo, D. R. Corbin, A. Navrotsky, *J. Phys. Chem. C* **2018**, *122*, 20366.
[35] Y.-K. Ma, S. Rigolet, L. Michelin, J.-L. Paillaud, S. Mintova, F. Khoerunnisa, T. J. Daou, E.-P. Ng, *Microporous Mesoporous Mater.* **2021**, *311*, 110683.
[36] H. Sanaeishoar, M. Sabbaghan, F. Mohave, *Microporous Mesoporous Mater.* **2015**, *217*, 219.
[37] P. Morales-Pacheco, F. Alvarez, L. Bucio, J. M. Domínguez, *J. Phys. Chem. C* **2009**, *113*, 2247.
[38] M. Handke, M. Kwaśny, *Vib. Spectrosc.* **2014**, *74*, 127.
[39] E. F. T. Lee, L. V. C. Rees, *J. Chem. Soc. Faraday Trans. 1 Phys. Chem. Condens. Phases* **1987**, *83*, 1531.
[40] H. Kosslick, R. Fricke, In *Characterization II* (Eds.: Karge, H. G.; Weitkamp, J.), Springer, Berlin, Heidelberg, **2007**, pp. 1–66.
[41] G. Engelhardt, D. Michel, **1987**.
[42] S. Ramdas, J. Klinowski, *Nature* **1984**, *308*, 521.
[43] R. F. Pettifer, R. Dupree, I. Farnan, U. Sternberg, *J. Non-Cryst. Solids* **1988**, *106*, 408.
[44] F. Mauri, A. Pasquarello, B. G. Pfrommer, Y.-G. Yoon, S. G. Louie, *Phys. Rev. B* **2000**, *62*, R4786.
[45] P. Bodart, J. B. Nagy, G. Debras, Z. Gabelica, P. A. Jacobs, *J Phys Chem U. S.* **1986**, *90:21*.
[46] E. Dib, I. M. Costa, G. N. Vayssilov, H. A. Aleksandrov, S. Mintova, *J. Mater. Chem. A* **2021**, *9*, 27347.
[47] F. Dubray, E. Dib, I. Medeiros-Costa, C. Aquino, D. Minoux, S. van Daele, N. Nesterenko, J.-P. Gilson, S. Mintova, *Inorg. Chem. Front.* **2022**, *9*, 1125.
[48] D. Massiot, F. Fayon, M. Capron, I. King, S. Le Calvé, B. Alonso, J.-O. Durand, B. Bujoli, Z. Gan, G. Hoatson, *Magn. Reson. Chem.* **2002**, *40*, 70.

A new post-synthetic hydrothermal treatment method is developed to alter the atomic orders of nanosized chabazite (CHA) zeolites. This method allows simultaneous dealumination and silylation of CHA to tune the Si/Al ratio from 2 to 4 by altering the acidity and concentration of the added silicon source. Moreover, distribution and concentration of silanol sites were also altered during the treatment.

S. Ghojavand, E. Dib, B. Riodent, A. Magisson, V. Ruaux, S. Mintova*

Altering the atomic order in nanosized CHA zeolites by post-synthetic treatments

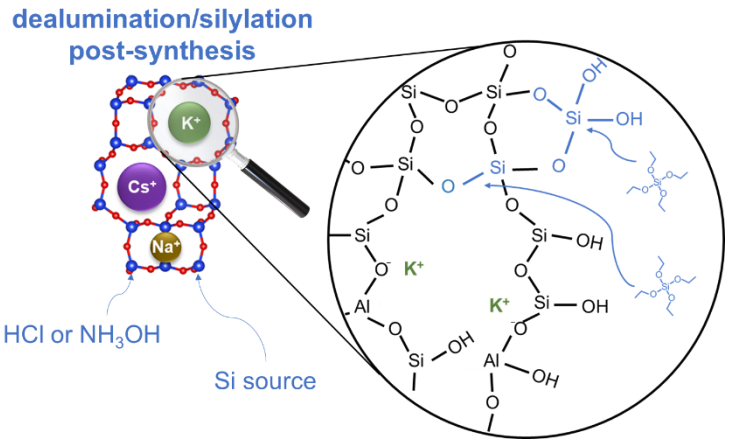

Supporting Information

Altering the atomic order in nanosized CHA zeolites by post-synthetic treatments

Sajjad Ghojavand, Eddy Dib, Baptiste Riodent, Aymeric Magisson, Valérie Ruaux, Svetlana Mintova[*]

Table S1. Concentration of silanol sites based on the FTIR and ^{1}H MAS NMR spectroscopy, molar absorption coefficients, and the chemical formula of reference, CHA-pH8.5-2Si, CHA-pH8.5-4Si, CHA-pH2.4-2Si, CHA-pH2.4-4Si, CHA-pH1.0-2Si, and CHA-pH1.0-4Si nanosized CHA samples.

Sample	$[OH]_{FTIR}$	$[OH]_{NMR}$	ε_{OH} [a]	Chemical formula
	$cm^{-1}\ g^{-1}$	$mmol\ g^{-1}$	$cm\ mmol^{-1}$	(ICP-MS)
Reference	644	3.43	382	$Na_{1.8}K_{5.7}Cs_{4.0}Al_{11.1}Si_{24.8}O_{72}$
CHA-pH8.5-2Si	1296	3.99	652	$H_{1.9}Na_{0.3}K_{4.3}Cs_{2.8}Al_{9.3}Si_{25.1}O_{72}$
CHA-pH8.5-4Si	1427	4.14	650	$H_{3.2}K_{3.7}Cs_{2.4}Al_{9.2}Si_{26.8}O_{72}$
CHA-pH2.4-2Si	1756	5.62	628	$H_{1.8}Na_{0.2}K_{4.7}Cs_{3.2}Al_{10.0}Si_{24.5}O_{72}$
CHA-pH2.4-4Si	1743	5.60	626	$H_{2.3}K_{4.0}Cs_{2.7}Al_{9.0}Si_{26.8}O_{72}$
CHA-pH1.0-2Si	3331	6.61	1013	$H_{3.3}K_{1.9}Cs_{2.5}Al_{7.7}Si_{29.1}O_{72}$
CHA-pH1.0-4Si	2831	6.36	895	$H_{2.6}K_{2.4}Cs_{2.3}Al_{7.3}Si_{29.3}O_{72}$

a) The molar absorption coefficients (ε_{OH}) are calculated using $\varepsilon_{OH} = [OH]_{FTIR}.S/[OH]_{NMR}$ and S is the area of FTIR pellets (2.01 cm^2).

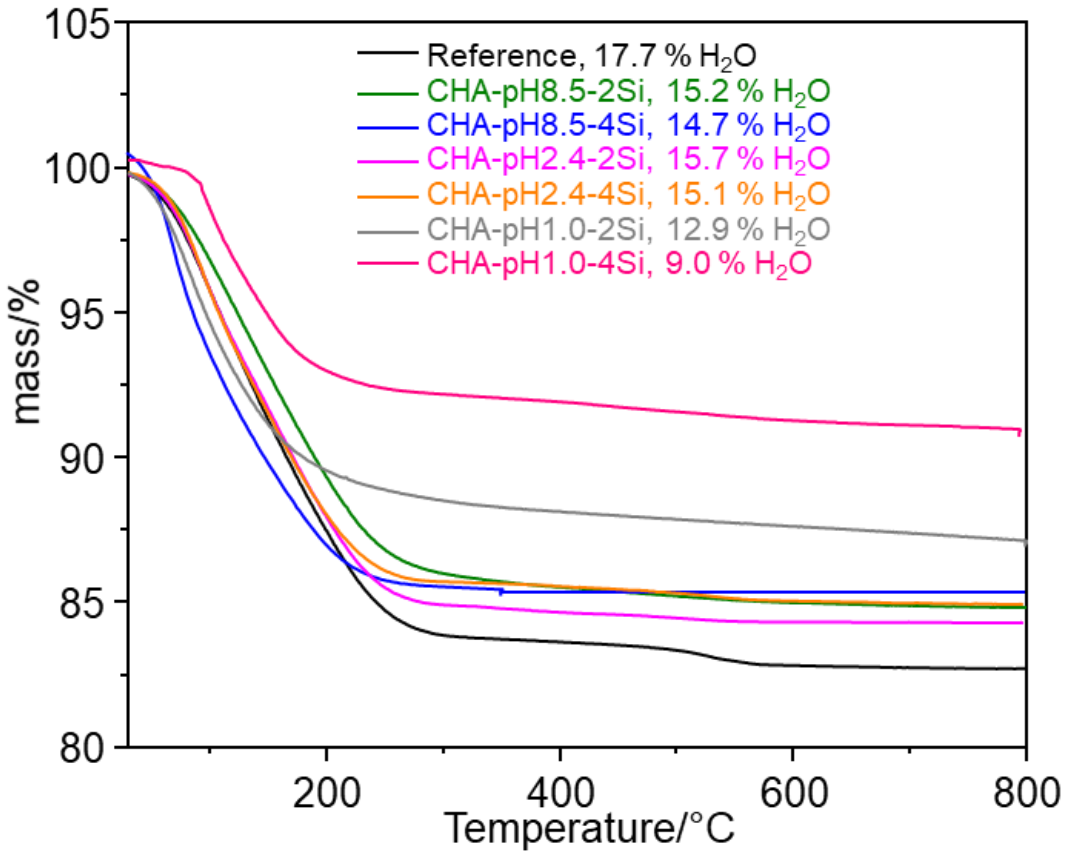

Figure S1. Thermal gravimetric analysis of reference, CHA-pH8.5-2Si, CHA-pH8.5-4Si, CHA-pH2.4-2Si, CHA-pH2.4-4Si, CHA-pH1.0-2Si, and CHA-pH1.0-4Si nanosized CHA samples.

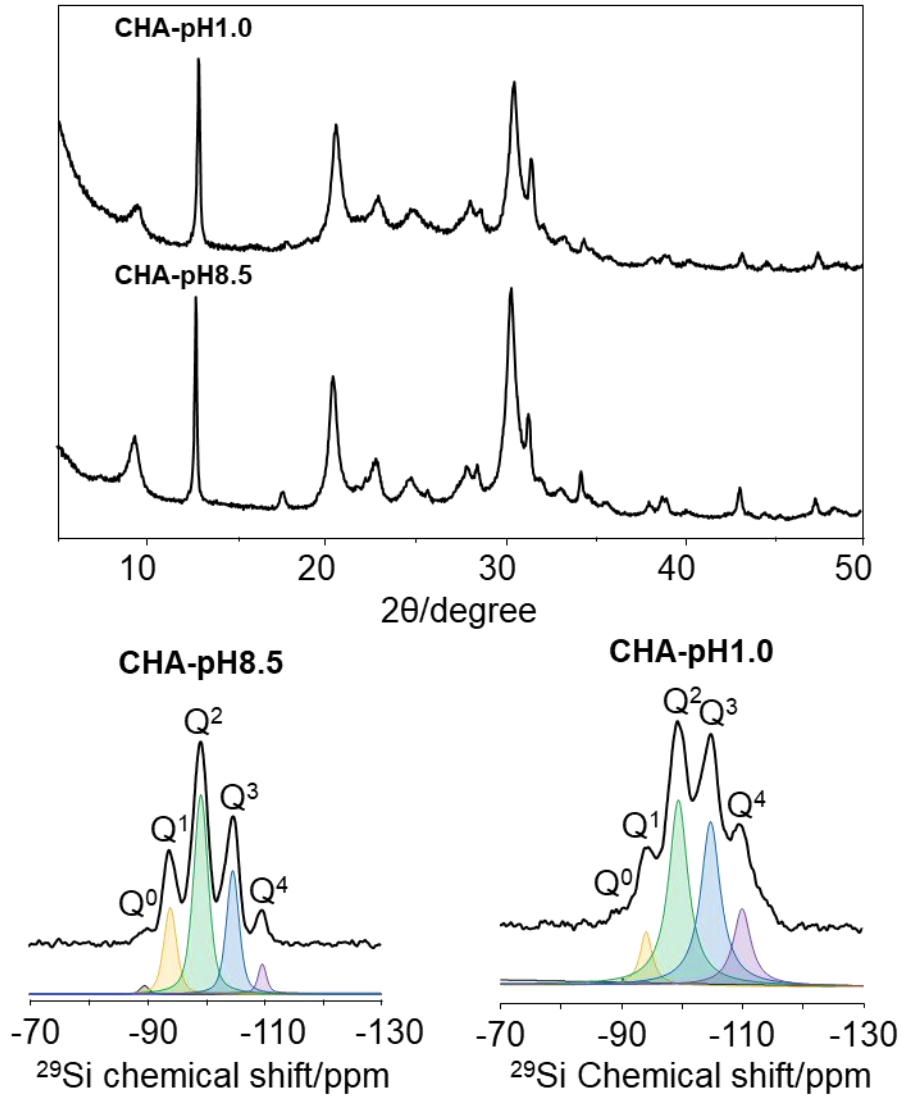

Figure S2. XRD patterns and ^{29}Si MAS NMR spectra of CHA-pH8.5 and CHA-pH1.0 nanosized CHA samples. Color code: black for Q^0, yellow for Q^1, green for Q^2, blue for Q^3, and purple for Q^4 species.

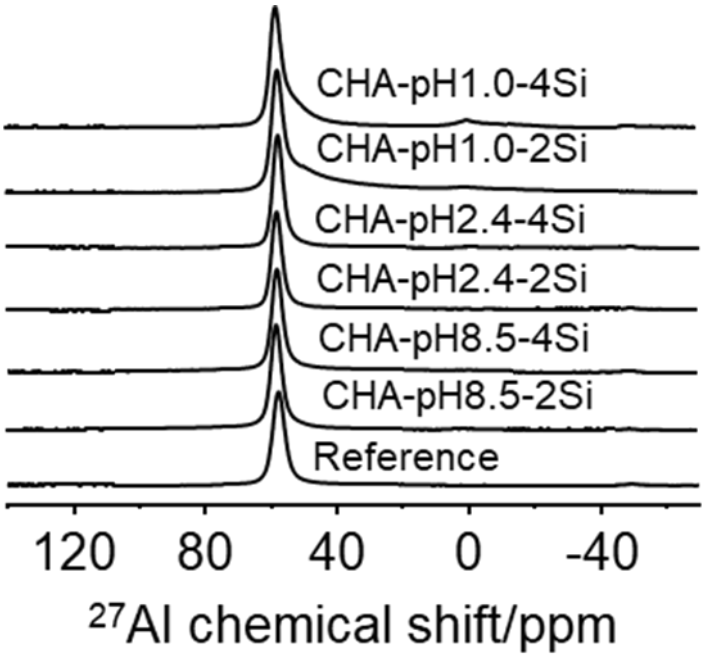

Figure S3. ^{27}Al MAS NMR spectra of nanosized CHA reference, CHA-pH8.5-2Si, CHA-pH8.5-4Si, CHA-pH2.4-2Si, CHA-pH2.4-4Si, CHA-pH1.0-2Si, and CHA-pH1.0-4Si samples.

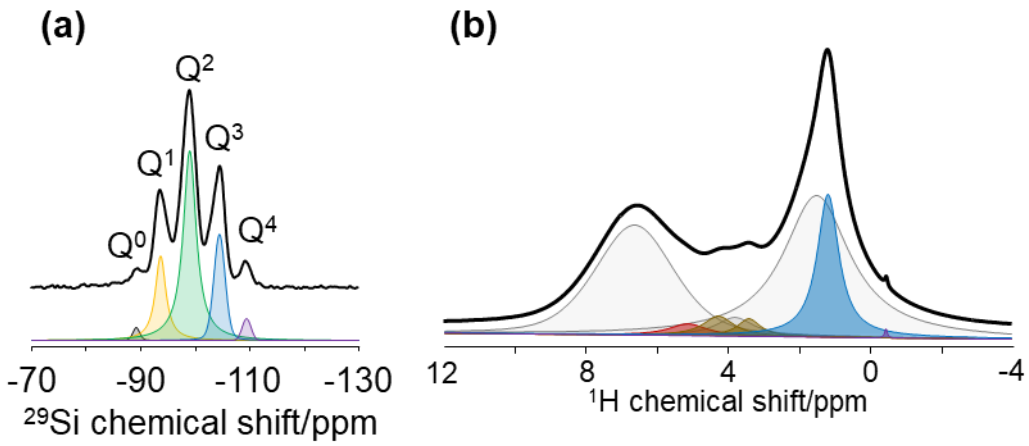

Figure S4. (a) ^{29}Si and (b) ^{1}H MAS NMR spectra of the nanosized CHA reference sample.

Table S2. Deconvolution parameters of reference, CHA-pH8.5, CHA-pH1.0, CHA-pH8.5-2Si, CHA-pH8.5-4Si, CHA-pH2.4-2Si, CHA-pH2.4-4Si, CHA-pH1.0-2Si, and CHA-pH1.0-4Si nanosized CHA samples.

Sample	Q^0/%	Q^1/%	Q^2/%	Q^3/%	Q^4/%
Reference	1	20	56	20	3
CHA-pH8.5	1	19	49	26	4
CHA-pH1.0	0	8	41	36	15
CHA-pH8.5-2Si	1	14	46	25	14
CHA-pH8.5-4Si	0	10	43	26	21
CHA-pH2.4-2Si	0	18	44	34	4
CHA-pH2.4-4Si	0	9	41	32	18
CHA-pH1.0-2Si	2	3	30	32	33
CHA-pH1.0-4Si	0	4	30	29	37

Table S3. ^{1}H MAS NMR deconvolutions of reference, CHA-pH8.5-2Si, CHA-pH8.5-4Si, CHA-pH2.4-2Si, CHA-pH2.4-4Si, CHA-pH1.0-2Si, and CHA-pH1.0-4Si zeolite samples.

Reference	^{1}H chemical shift/ppm	-0.5	1.2	3.5	4.2	5.2
	Concentration/mmol g^{-1}	0.02	2.30	0.30	0.46	0.35
CHA-pH8.5-2Si	^{1}H chemical shift/ppm	-0.5	1.3	3.4	4.5	-
	Concentration/mmol g^{-1}	0.02	2.87	0.92	0.18	-
CHA-pH8.5-4Si	^{1}H chemical shift/ppm	-	1.4	3.3	3.5	-
	Concentration/mmol g^{-1}	-	2.69	0.67	0.78	-
CHA-pH2.4-2Si	^{1}H chemical shift/ppm	-	1.3	2.2	3.2	-
	Concentration/mmol g^{-1}	-	3.43	0.34	1.85	-
CHA-pH2.4-4Si	^{1}H chemical shift/ppm	-	0.8	1.5	3.3	-
	Concentration/mmol g^{-1}	-	0.37	3.11	2.12	-
CHA-pH1.0-2Si	^{1}H chemical shift/ppm	-	0.8	1.5	2.0	3.6
	Concentration/mmol g^{-1}	-	0.11	2.79	2.77	0.94
CHA-pH1.0-4Si	^{1}H chemical shift/ppm	-	0.9	1.5	2.1	3.5
	Concentration/mmol g^{-1}	-	0.14	2.53	3.09	0.60

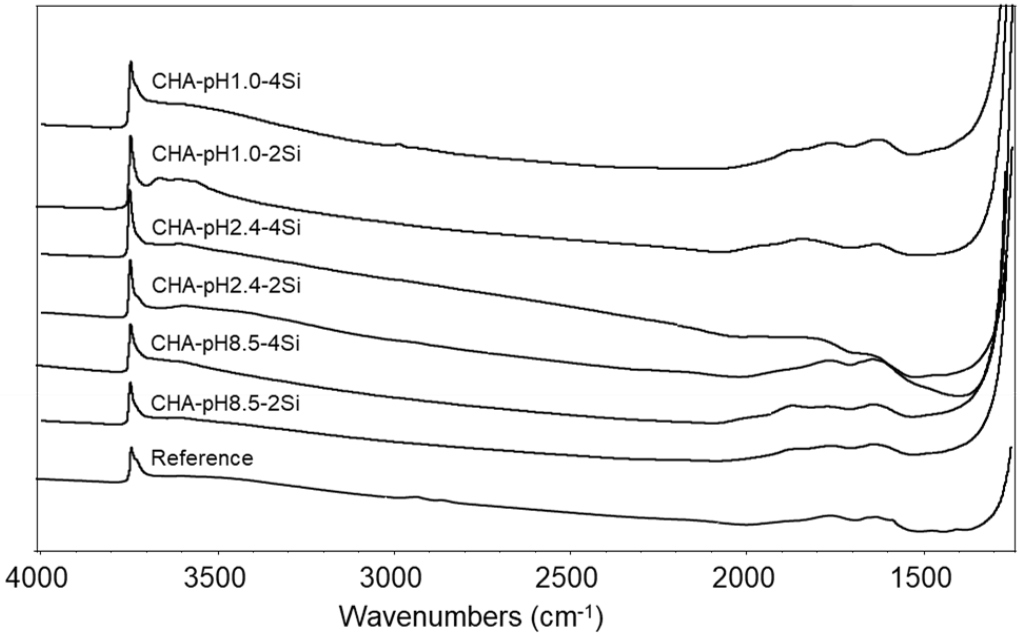

Figure S5. FTIR spectra of reference, CHA-pH8.5-2Si, CHA-pH8.5-4Si, CHA-pH2.4-2Si, CHA-pH2.4-4Si, CHA-pH1.0-2Si, and CHA-pH1.0-4Si nanosized CHA samples.

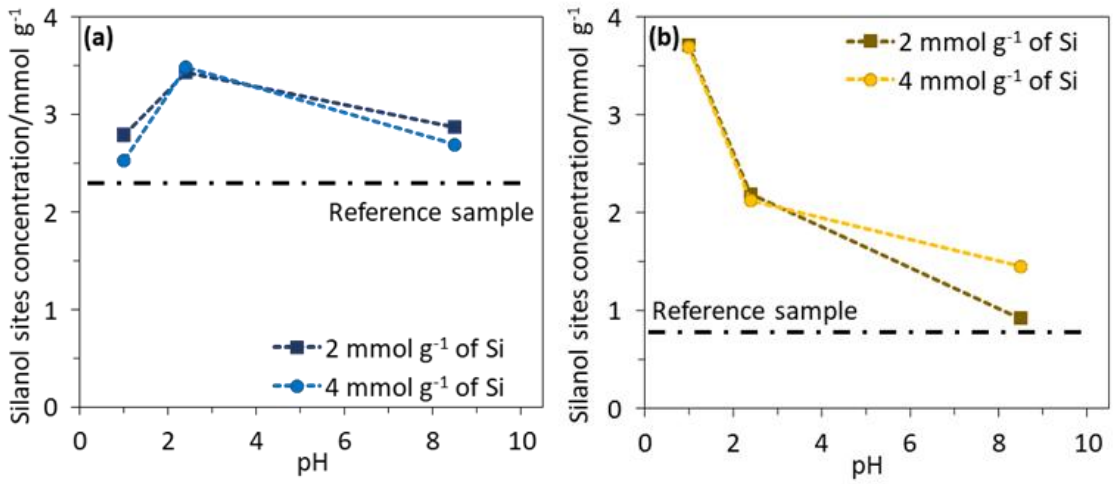

Figure S6. The changes in the concentration of silanol sites for a) isolated and weakly hydrogen bonded and b) moderately hydrogen bonded versus the pH and Si concentration during the post-synthetic treatment of nanosized CHA based on ^{1}H MAS NMR spectroscopy.